

# Magnetic properties and magnetocaloric effect of DyCo<sub>9</sub>Si<sub>4</sub>

Naohito Tsujii<sup>1</sup>, Atsushi Miyake<sup>2,3</sup>, Masashi Tokunaga<sup>2</sup>, Jaroslav Valenta<sup>1,4</sup>, Hiroya Sakurai<sup>1</sup>

<sup>1</sup> Research Center for Materials Nanoarchitectonics, National Institute for Materials Science, 1-2-1 Sengen, Tsukuba, Ibaraki 305-0047, Japan

<sup>2</sup> Institute for Solid State Physics, the University of Tokyo, Kashiwa, Chiba 277-8581, Japan

<sup>3</sup> Institute for Materials Research, Tohoku University, Narita cho 2145-2, Oarai, Ibaraki 311-1313, Japan

<sup>4</sup> Institute of Physics, Czech Academy of Sciences, Na Slovance 2, 182 21 Prague 8, Czech Republic

Polycrystalline samples of DyCo<sub>9</sub>Si<sub>4</sub> with the tetragonal LaFe<sub>9</sub>Si<sub>4</sub>-type structure have been synthesized by arc melting and high-temperature annealing. Results of the magnetization  $M$  and specific heat  $C_p$  measurements show the existence of two magnetic anomalies at  $T_C = 40$  K and  $T_m = 20$  K. The transition at  $T_C = 40$  K is attributed to the ferromagnetic transition of the Co sublattice. The magnetic moments of Dy<sup>3+</sup> appear to align gradually below  $T_C$ , and almost fixed below  $T_m$ , at which a broad maximum in  $C_p$  has been observed. Field-dependent  $M$  at  $T = 2$  K up to  $H = 7$  T suggested that the magnetic moment of Dy<sup>3+</sup> is coupled antiferromagnetically with those of Co, forming a ferrimagnetic structure. Magnetization measurements up to 50 T at low temperatures using a pulse magnet demonstrated a spin-flip transition around  $H = 20$  T, above which the magnetic moments of Co and Dy are in parallel. The spin-flip transition becomes broad with increasing temperature but still remains at  $T_C = 40$  K, indicating a strong antiparallel coupling between Co and Dy moments even in the paramagnetic state. The magnetocaloric effect was evaluated from  $C_p$  and  $M$ , and also from the sample-temperature variation in the quasi-adiabatic process with the pulsed magnetic field. The maximum entropy change for the field change from 5 to 0 T was observed at around  $T = T_m$  with the value  $\Delta S = 5$  J/kg K. The maximum temperature of  $\Delta S$  shifts to higher temperatures in high magnetic fields, resulting in the large value of  $\Delta S = 24$  J/kg K at  $T \sim T_C$  by the field change from 50 to 0 T. The present results demonstrate that the pulsed-field measurement is a powerful method to evaluate the magnetocaloric effect of materials.

key word: DyCo<sub>9</sub>Si<sub>4</sub>, intermetallic compound, magnetization, magnetocaloric effect

## Introduction

Intermetallic compounds with rare-earth elements and transition metals are industrially of great importance for permanent magnets, hydrogen absorption alloys, magnetocaloric materials, and so on. Special attention has recently been paid to low-temperature magnetocaloric effect of rare-earth intermetallic compounds because of the need to liquefy hydrogen as energy media. This calls for materials with large magnetic-entropy change in the temperature range between 77 and 20 K, which are the liquefaction temperatures of nitrogen and hydrogen at ambient pressure, respectively. Promising series of compounds include the Laves phase  $RCO_2$  ( $R$  being a rare-earth element) with the cubic  $MgCu_2$ -type structure.  $HoCo_2$  and  $ErCo_2$ , for examples, exhibit a first-order magnetic transition at  $T_C = 83$  K and 37 K, respectively [1]. Applying magnetic fields results in the shift of  $T_C$  to higher temperatures, causing a sharp and significant field-induced magnetic-entropy change around  $T_C$ . Thanks to these characteristic magnetic properties, the  $RCO_2$ -type compounds are considered one of the best candidates for the magnetic refrigeration materials [2]. The peculiar magnetic properties in the  $RCO_2$  compounds stem from the itinerant-electron metamagnetism due to the Co-3d electrons [3]. Indeed, the iso-structural  $YCo_2$  and  $LuCo_2$  without magnetic moments at the  $R$  site show enhanced Pauli-paramagnetic behavior and exhibit an itinerant-electron metamagnetic transition at  $H_C = 69$  and 74 T, respectively [3]. Thus, the coupling of local magnetic moments of  $R$  elements with the field-induced metamagnetic behavior of itinerant 3d-electrons plays an essential role in the outstanding magnetic properties in the  $RCO_2$  compounds.

In this regard, the  $RCO_9Si_4$ -type compound is another candidate for interesting and useful magnetic intermetallic compounds.  $RCO_9Si_4$  crystallizes in the tetragonal  $LaFe_9Si_4$ -type structure with the space group  $I 4/m c m$ . Isostructural compounds have been reported to show wide range of interesting phenomena. For example,  $LaFe_{13-x}Si_x$  shows field-induced metamagnetism and is expected to be useful for the middle-temperature magnetic refrigeration applications [4, 5].  $YbCu_9Sn_4$  demonstrates rattling behavior of the Yb ions inside the cage framework structure [6].  $RCO_9Si_4$  compounds are especially interesting for the low-temperature magnetic properties.  $LaCo_9Si_4$  shows an enhanced Pauli-paramagnetic behavior down to the lowest temperatures with a maximum in the magnetic susceptibility at  $T_{max} = 20$  K, and exhibits an itinerant-electron metamagnetic transition with  $H_C = 3.5$  T at low temperatures [7]. This compound has been characterized to be a nearly-ferromagnetic metal in the vicinity of the ferromagnetic quantum critical point (QCP) from the NMR measurements and the analyses based on the spin-fluctuation theory [8]. Indeed, the isostructural compound  $YCo_9Si_4$  undergoes a weak ferromagnetic order at 25 K [9]. For the cases of magnetic  $R$  elements,  $CeCo_9Si_4$  appears to be a normal Pauli-paramagnetic metal because of the strong hybridization between Ce-4f and Co-3d electrons [10],

while  $RCo_9Si_4$  with  $R = Pr, Nd, Sm, Gd,$  and  $Tb$  exhibit ferrimagnetic transition [11].  $PrCo_9Si_4$  and  $NdCo_9Si_4$  were reported to exhibit a first-order ferromagnetic transition [12], although this appears to depend on samples [13]. In addition,  $GdCo_9Si_4$  has been reported to show a distinct magnetocaloric effect, as characterized by a large magnetic entropy change  $\Delta S_m = 24 \text{ J/kg K}$  for the magnetic field change from 5 to 0 T [14], which is comparable to that in  $HoCo_2$  [1]. Hence, the properties of  $RCo_9Si_4$  are very similar to those of  $RCO_2$  compounds.

This motivated us to start the research on  $DyCo_9Si_4$ . In general, rare-earth compounds with heavy rare-earth elements ( $Tb, Dy, Ho, Er, Tm$ ) are suitable for magnetic cooling applications rather than light rare-earth compounds. This is mainly because of larger magnetic moments and relatively narrower crystalline-electric field splitting in heavy rare-earth elements than those in light rare-earth, which allows us to exploit larger entropy change by magnetic field [15]. Although the existence of  $DyCo_{13-x}Si_x$  phase has been known [16, 17], a stoichiometric compound  $DyCo_9Si_4$  has not been obtained, thereby its magnetic and electrical properties have not been investigated so far. In this paper, we report for the first time the physical properties of  $DyCo_9Si_4$ . A pure  $DyCo_9Si_4$  phase has been stabilized. Temperature dependence of the magnetization, electrical resistivity, and specific heat have been investigated with and without magnetic fields. Furthermore, we studied the magnetization by pulsed magnetic fields up to 50 T, and the concomitant temperature change by field was also measured.

### Experimental Procedure

Polycrystalline sample of  $DyCo_9Si_4$  has been synthesized by arc melting and subsequent annealing. Pure elements of Dy (99.9%), Co (99.99%), and Si (99.999%) were weighted to make a stoichiometric compound and melted by an arc furnace under an argon atmosphere. The melted ingot was turned over and melted again to ensure homogeneity. This process was repeated for several times. After the arc melting, the weight decrease was less than 1%. The melted ingot was wrapped with a tantalum foil and sealed in a quartz tube under argon. The tube was heated in an electric furnace for annealing. The sample was annealed at 1323 K for 12 days.

Samples were characterized by a powder X-ray diffraction (XRD) and a scanning electron microscope (SEM). Powder XRD data were collected by a  $Cr K\alpha$ -radiation with the wavelength of  $\lambda = 2.2899 \text{ \AA}$  using a Rigaku Mini-Flex diffractometer. The diffraction data were analyzed with the Full-Prof suite software. SEM data were obtained on a polished  $DyCo_9Si_4$  surface with a JSM-6500F from the JEOL company. Chemical compositions are evaluated by using the energy dispersive spectroscopy (EDS).

Magnetic properties were investigated using an MPMS3, Quantum Design, Co., in the temperature range from 2 to 300 K and the field range up to 5 T. Furthermore, magnetization up to 50 T were measured in a pulsed magnetic field with a 36-msec duration at the Institute for Solid

State Physics, the University of Tokyo. Magnetization was measured by a conventional induction method. For the measurements below 4.2 K, the sample space was immersed in liquid He. On the other hand, the sample was kept in He gas at  $T > 4.2$  K. Because of the limited cooling power of the He gas and the short time duration of the applied magnetic field, the magnetization process can be in quasi-adiabatic conditions. Therefore, sample temperatures may change as a function of the magnetic field due to the magnetocaloric effect. To evaluate the field variation of the temperature, we measured the sample temperature and magnetization simultaneously. The temperature during the magnetization process was measured by a homemade capacitance thermometer using a ferro-electric  $\text{KTa}_{1-x}\text{Nb}_x\text{O}_3$  crystal attached to the sample with Apiezon N grease. Details of the measurements were published previously [18, 19]. Electrical resistivity and specific heat were measured by a PPMS, Quantum Design Co.

### Results and discussion

In Fig. 1, powder XRD patterns of the as-cast and the annealed samples of  $\text{DyCo}_9\text{Si}_4$  are shown. While the pattern of the as-cast sample is of multi-phases, that of the annealed sample agrees well with the calculation for the tetragonal  $\text{LaFe}_9\text{Si}_4$ -type structure. The Rietveld fitting suggested that the Co and Si atoms are almost ordered. The lattice parameters are obtained by the fitting to be  $a = 7.7477(1)$  Å and  $c = 11.4791(3)$  Å. The chemical composition evaluated by the SEM-EDS is in agreement with the formula  $\text{DyCo}_9\text{Si}_4$  (see Fig. S1 in the *Supporting Information Figures*).

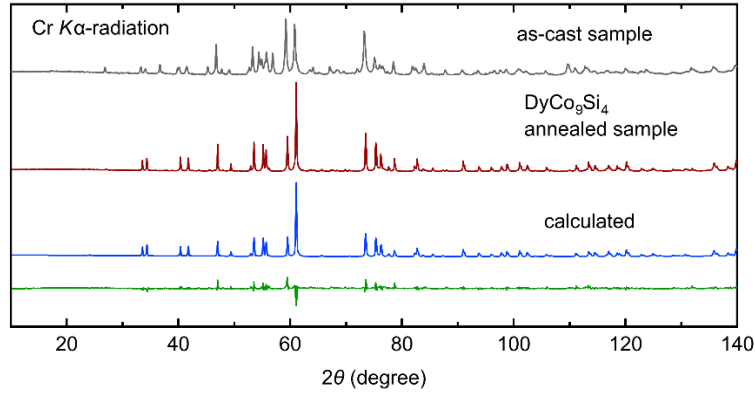


Fig. 1 Powder X-ray diffraction patterns of the  $\text{DyCo}_9\text{Si}_4$  as-cast and annealed samples

In Fig. 2 (a), magnetic susceptibility  $M/H$  of the  $\text{DyCo}_9\text{Si}_4$  annealed sample and its inverse as functions of temperature are shown. The  $M/H$  increases rapidly below  $T_C = 40$  K, suggesting a magnetic transition. Above  $T_C$ , the  $M/H$  was fitted with a Curie-Weiss function,  $M/H = C/(T - \theta) + \chi_0$ , where  $C$ ,  $\theta$ ,  $\chi_0$  are the Curie constant, the Weiss temperature, and a temperature independent term, respectively. A fitting for the temperature range from 150 to 300 K yielded the values  $C = 16.40$  emu K/mol,  $\theta = -6.9$  K, and  $\chi_0 = 0.031$  emu/mol. The relatively large value of  $\chi_0$  can be due

to the contribution of Co-3d electrons with a large density of states at the Fermi energy, which is suggested from the electronic specific heat coefficient, as shown later. The Curie constant is described as  $C = Np_{\text{eff}}^2/3k_B$ , where  $N$  is the number of magnetic ions,  $p_{\text{eff}}$  the effective magnetic moment, and  $k_B$  the Boltzmann constant. The value  $C = 16.40$  emu K/mol corresponds to  $p_{\text{eff}} = 11.45\mu_B$  per formula unit. This is somewhat larger than that expected for a free  $\text{Dy}^{3+}$  ion,  $10.63\mu_B$ , suggesting non negligible contribution of the Co magnetic moments. In  $\text{DyCo}_9\text{Si}_4$ , there are 3 crystallographic Co sites; 4 Co ions at the  $16k$  position, 4 Co at the  $16l$ , and a Co at the  $4d$  position. For the case of  $\text{LaCo}_9\text{Si}_4$ , the band structure calculation predicts that the magnetic moment of the Co ions mainly occurs at the  $16k$  site [7]. If we assume that the  $\text{Dy}^{3+}$  has a local moment with  $p_{\text{Dy}} = 10.63\mu_B$ , and the 4 Co ions at the  $16k$  position also have magnetic moments, magnetic moments of the Co,  $p_{\text{Co}}$  can be estimated by  $p_{\text{eff}}^2 = p_{\text{Dy}}^2 + 4p_{\text{Co}}^2$ , yielding  $p_{\text{Co}} = 1.81 \mu_B$  per Co ion at the  $16k$  site. This value is close to that of  $s = 1/2$  and  $g = 2$ ,  $p_{\text{eff}} = 1.73 \mu_B$ . Similar value of  $p_{\text{Co}}$  has been reported for  $\text{GdCo}_9\text{Si}_4$  as well, where Co atoms at the  $16k$  site were assumed to be magnetic [20].

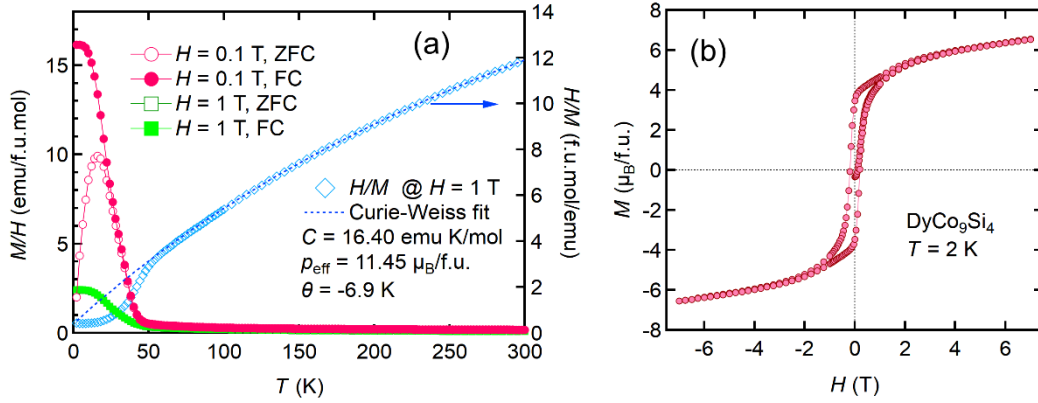


Fig. 2 (a) Temperature dependence of the magnetic susceptibility  $M/H$  and its inverse  $H/M$  of  $\text{DyCo}_9\text{Si}_4$  annealed sample. Dotted line indicates the result of fitting with a Curie-Weiss function. (b) Field dependence of the magnetization  $M$  measured at  $T = 2$  K.

The temperature dependence of  $M/H$  measured at  $H = 0.1$  T shows another anomaly around  $T_m = 20$  K, where the data for zero-field cooled (ZFC) and field-cooled (FC) measurements start to deviate. This anomaly is broad and is not likely to be due to a long-range magnetic ordering. The origin of this anomaly will be discussed later.

In Fig. 2 (b), the field dependence of the magnetization measured at  $T = 2$  K is shown. A clear ferromagnetic-like curve with a hysteresis is observed. However, the saturation magnetic moment is about  $6 \mu_B$  per formula unit, much smaller than that expected for a  $\text{Dy}^{3+}$  magnetic moment. If we neglect the crystalline electric field (CEF) effect, the  $\text{Dy}^{3+}$  ion has a total angular momentum of  $J = 15/2$  and the Landé's  $g$ -factor  $g = 4/3$ , which leads to a saturation moment  $gJ_z = 10 \mu_B$  for a  $\text{Dy}^{3+}$  ion. Here, let us assume that the 4 Co ions at the  $16k$  site have the spin  $s = 1/2$  with  $g = 2$ ,

and those magnetic moments point to the opposite direction with respect to that of  $\text{Dy}^{3+}$  ion. Then, the magnetic moment due to the Co ions can be roughly estimated to be  $4 \times g_{\text{SZ}} = 4 \mu_{\text{B}}/\text{f.u.}$ , and the net magnetic moment of  $\text{DyCo}_9\text{Si}_4$  should be  $10 - 4 = 6 \mu_{\text{B}}$  per formula unit. This is in good agreement with that observed at  $H = 5 \text{ T}$  and  $T = 2 \text{ K}$ , as seen in Fig. 2 (b). Although the accurate values should be modified because of the CEF splitting and the evaluation of Co magnetic moments, this result suggests that the magnetic moments of  $\text{Dy}^{3+}$  and Co are coupled in the opposite way. Such ferri-magnetic structures were suggested for the isostructural  $\text{GdCo}_9\text{Si}_4$  [20] and  $\text{TbCo}_9\text{Si}_4$  [21], and were confirmed by the observation of the step-like increase in the magnetization at around 30 T, above which the magnetization appears to saturate to the sum of Co and  $\text{Gd}^{3+}/\text{Tb}^{3+}$  moments.

Field dependence of the magnetization for the weak field region has been measured in detail, which is shown in Fig. S2 (a) (see the *Supporting Information Figures*). All the magnetization processes show linear field dependence for fields above 0.5 T. By extrapolating the data of  $H > 0.5 \text{ T}$  to the zero-field by a linear fitting, the saturation magnetization,  $M_{\text{sat}}$ , has been estimated, and is displayed as a function of  $T$  in Fig. S2 (b). The value of  $M_{\text{sat}}$  starts to increase at 40 K, indicating a ferromagnetic transition occurs at  $T_{\text{C}} = 40 \text{ K}$ . While  $M_{\text{sat}}$  increases with decreasing  $T$  below  $T_{\text{C}}$ , a shoulder-like hump is seen around  $T = 20 \text{ K}$ . This temperature corresponds to  $T_{\text{m}}$ , where the magnetizations of ZFC and FC processes start to split. This is attributed to the onset of ordering of the Dy magnetic moment, which aligns antiferromagnetically with that of the Co. The first transition at  $T_{\text{C}} = 40 \text{ K}$  is due to the itinerant-electron ferromagnetism of Co-3d electrons. The second anomaly at  $T_{\text{m}} = 20 \text{ K}$  is rather broad. It is hence not a long-range ordering but is more likely to be a short-range order such as spin freezing. The separation of the  $M/H$  between ZFC and FC data below  $T_{\text{m}}$  in Fig. 2 (a) is consistent with this scenario.

In Fig. 3, temperature dependence of the electrical resistivity  $\rho$  of  $\text{DyCo}_9\text{Si}_4$  is shown. The resistivity shows a rapid decrease at  $T_{\text{C}} = 40 \text{ K}$ . This anomaly is significantly suppressed in magnetic field, as seen in Fig. 3 (b). This is consistent with the ferromagnetic transition. While the  $\rho$ - $T$  curve does not show a clear anomaly at around  $T_{\text{m}} = 20 \text{ K}$ , a broad peak is seen in its temperature derivative  $d\rho/dT$ , shown in Fig. 3 (c).

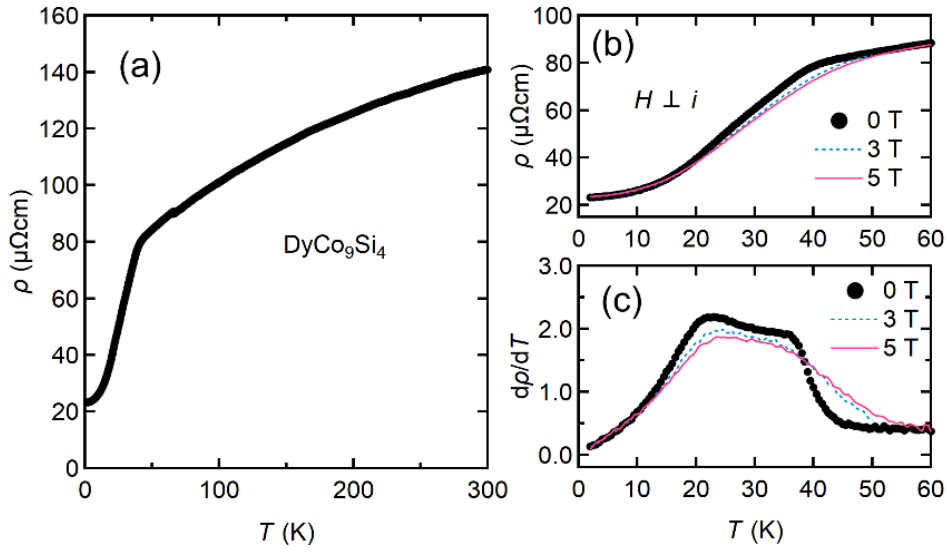


Fig. 3 Temperature dependence of the electrical resistivity  $\rho$  of  $\text{DyCo}_9\text{Si}_4$  (a), low temperature part with its magnetic field dependence (b), and the temperature derivative  $d\rho/dT$  (c).

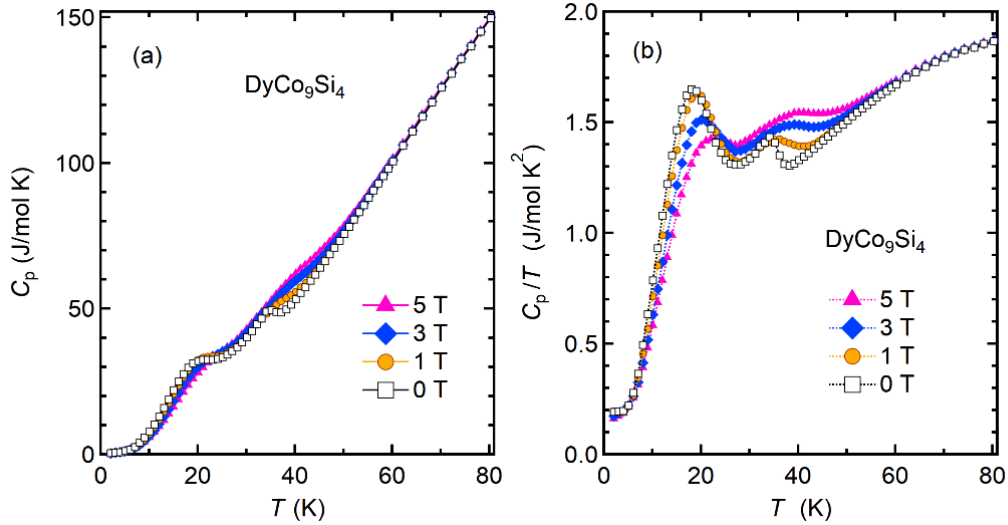


Fig. 4 Temperature dependence of the specific heat  $C_p$  of  $\text{DyCo}_9\text{Si}_4$  measured under magnetic fields of  $H = 0, 1, 3,$  and  $5$  T (a), and temperature dependence of  $C_p/T$  (b).

Fig. 4 displays temperature dependence of the specific heat  $C_p$  (a), and  $C_p/T$  of  $\text{DyCo}_9\text{Si}_4$  (b). In zero magnetic field, two anomalies are observed at  $T_C = 40$  K and  $T_m = 20$  K. At 40 K,  $C_p$  shows a jump, corresponding to the ferromagnetic ordering. This is consistent with the temperature dependence of the  $M_{\text{sat}}$  (Fig. S2 (b)), where the saturation magnetic moment  $M_{\text{sat}}$  continuously decreases with  $T$  until it reaches zero at  $T_C = 40$  K. For the data at  $H > 0$  T, the peak in  $C_p$  at  $T_C$

becomes broad, shifting to higher temperatures, consistent with the ferromagnetic nature. The  $C_p$  anomaly at 40 K is rather small without a divergent behavior, similarly to the case in  $\text{GdCo}_9\text{Si}_4$  at  $T_C = 47$  K [20] and in  $\text{YCo}_9\text{Si}_4$  at  $T_C = 25$  K [9]. A small  $C_p$  anomaly at  $T_C$  without divergence is often the case for itinerant-electron ferromagnetic compounds, like  $\text{MnSi}$  [22],  $\text{SrRuO}_3$  [23],  $\text{Fe}_2\text{VAl}_{0.95}$  [24], and so on. The other anomaly at  $T_m = 20$  K is broader than that at  $T_C = 40$  K. From the analogy to the cases of  $\text{GdCo}_9\text{Si}_4$  [20], this broad peak corresponds to the gradual orientation of the  $\text{Dy}^{3+}$  magnetic moments by the internal field of Co. Nevertheless,  $C_p/T$  shows a relatively large peak at  $T_m = 20$  K. As the  $\text{Dy}^{3+}$  has a large orbital moment, it is possible that the alignment of the  $\text{Dy}^{3+}$  moment causes a distortion of the crystal lattice, which partly contribute to the  $C_p$  anomaly at 20 K. To elucidate if there are any phase transition at  $T_m$ , further experiments such as neutron diffraction measurements would be desired.

At low temperatures below 4 K,  $C_p/T$  becomes almost constant. In the case of Fermi-liquid systems, the relation  $C_p/T = \gamma + \beta T^2$  is observed, where  $\gamma$  and  $\beta$  are the electronic specific heat coefficient and a constant, respectively. In Fig. S4 in the supporting information, we show  $C_p/T$  as functions of  $T^2$ . In the figure, the Fermi-liquid relation is only seen at low temperatures below 4 K. Furthermore, the low temperature  $C_p/T$  in zero field shows a deviation from the Fermi liquid relation and exhibits slight enhancement. By applying magnetic field, this enhancement is suppressed and eventually the Fermi liquid behavior evolves at  $H = 5$  T. This indicates that the effect of spin fluctuation and/or any other magnetic contributions are involved in  $C_p/T$  at low temperature and low fields. Fitting of  $C_p/T$  data at  $H = 5$  T below 4 K yields the value of  $\gamma = 0.15$  J/Dy-mol  $\text{K}^2$ . A similar  $\gamma$  value is also reported for  $\text{LaCo}_9\text{Si}_4$ , where the large density of state due to the  $3d$  electrons plays the major role.

The entropy  $S$  of  $\text{DyCo}_9\text{Si}_4$  has been evaluated by integrating the  $C_p/T$  data over  $T$ . The temperature dependence of  $S_p$  in magnetic fields of 0, 1, 3, and 5 T have been plotted in Fig. S5 (a) (see *Supporting Information Figures*). By taking the difference from the zero-field data, the entropy change,  $\Delta S_p$ , has been evaluated and is shown in Fig. 5.

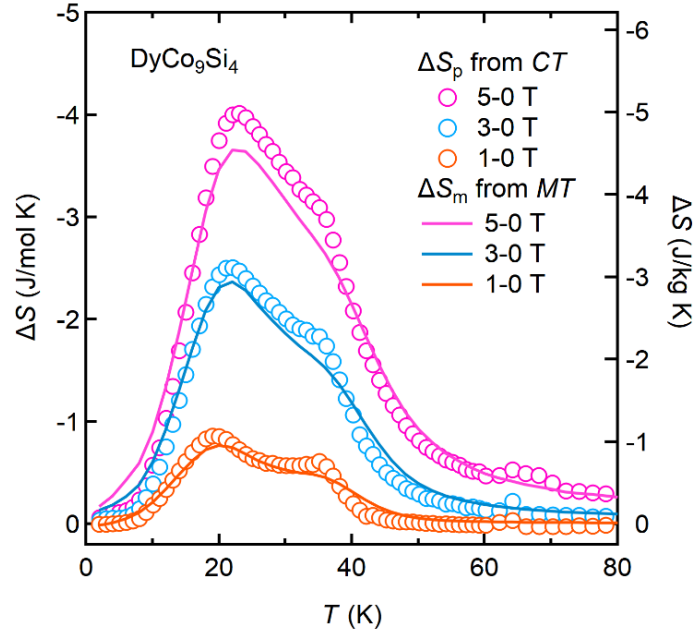


Fig. 5 Temperature dependence of the entropy change  $\Delta S$  of  $\text{DyCo}_9\text{Si}_4$  by magnetic field.

Here, the magnetic entropy change can also be calculated from the magnetization data by the Maxwell's relation,  $\Delta S_m = \int (\partial M / \partial T) dH$ . The magnetization data measured in various fields from 0.1 to 5 T are shown in Fig. S3 (Supporting Information Files). Using these data,  $\Delta S_m$  have been calculated and are plotted together with  $\Delta S_p$  in Fig. 5. It is noted that  $\Delta S_p$  and  $\Delta S_m$  agree each other. The maximum value of  $|\Delta S_p|$  is 4 J/mol K (or 5 J/kg K) for the magnetic-field change from 5 to 0 T, and 2.5 J/mol K (or 3 J/kg K) for the field change from 3 to 0 T. The  $|\Delta S_p|$  maximum is seen at  $T = 22$  K, which is close to  $T_m$ , indicating that the magnetic entropy related to the  $\text{Dy}^{3+}$  ion plays a major role in the magnetocaloric effect in  $\text{DyCo}_9\text{Si}_4$ . This is contrasting with the case of  $\text{GdCo}_9\text{Si}_4$  [14], where the largest  $\Delta S_m$  was observed at the onset of ferromagnetic transition,  $T_C$ . The absolute values of  $\Delta S_m$  in  $\text{GdCo}_9\text{Si}_4$  are also different from those in  $\text{DyCo}_9\text{Si}_4$ . A noticeably large magnetic entropy change,  $\Delta S_m = -24$  J/kg K with the field change from 5 to 0 T has been reported for  $\text{GdCo}_9\text{Si}_4$ . This value is 4 to 5 times as large as that in the present  $\text{DyCo}_9\text{Si}_4$ , although the magnetic properties look similar. It should be noted that in  $\text{GdCo}_9\text{Si}_4$ , the magnetic-entropy change shows a significant chemical-composition dependence [14]. Thus, the  $\Delta S_m$  value of  $\text{DyCo}_9\text{Si}_4$  may also be further enhanced by tuning the Co-Si chemical composition.

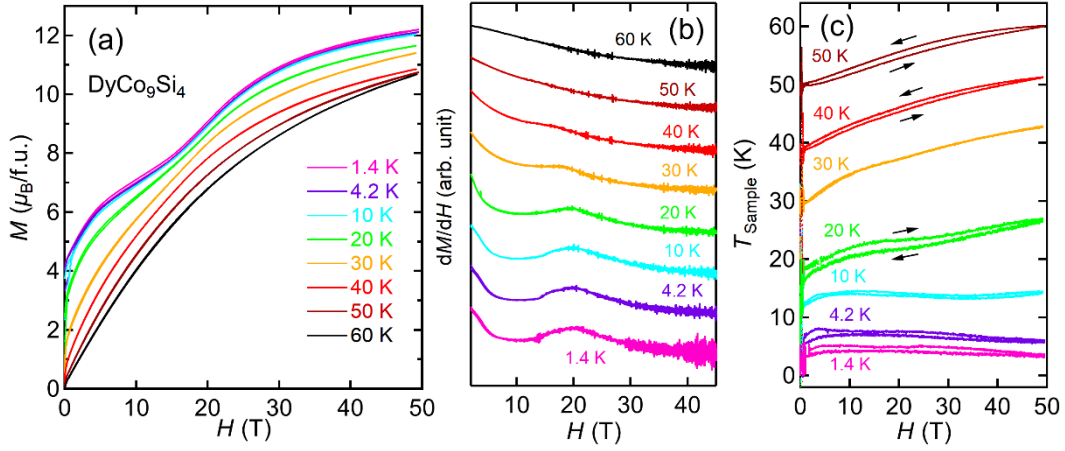


Fig. 6 Field dependence of the magnetization  $M$  of  $\text{DyCo}_9\text{Si}_4$  measured by pulsed magnetic fields (a), its field-derivative  $dM/dH$  (b), and the sample temperature (c). Values of the temperature shown in figures indicate the initial temperature just before the field scan.

In Fig. 6, magnetic properties in high magnetic-field are shown. Fig. 6 (a) shows the field dependence of the magnetizations  $M(H)$  measured by pulsed magnetic fields in various initial temperatures. Here, the initial temperature is measured at the beginning of the pulsed-field generation. Fig. 6 (b) shows the field derivative of magnetization,  $dM/dH$ . Fig. 6 (c) represents the temperature of the sample measured by a capacitance thermometer during the field sweep. The measurements with the initial temperature of  $T = 1.4$  and  $4.2$  K were carried out with the sample soaked in liquid helium, thereby the sample temperatures are supposed to be unchanged. Indeed, the measured temperature shown in Fig. 6 (c) indicates that this isothermal condition is almost preserved for  $T = 1.4$  and  $4.2$  K. The  $M(H)$  curve at  $T = 1.4$  K shows a step-like increase above  $H = 20$  T, suggesting a magnetic transition. From the magnetization results of Fig. 2, the magnetic structure at low fields has been considered to be a ferrimagnetic one, where the Co and Dy magnetic moments align in an antiparallel way. Above  $H = 30$  T, the  $M(H)$  tends to saturate to the value around  $12 \mu_B / \text{f.u.}$ , which is close to the effective magnetic moment estimated from the Curie-Weiss behavior of the magnetic susceptibility. Hence, the rapid increase in  $M(H)$  in  $\text{DyCo}_9\text{Si}_4$  around  $H = 20$  T is attributed to the change in the orientation of the magnetic moments from the antiparallel to a ferromagnetic configuration of Co and Dy magnetic moments in high fields. Similar magnetization behaviors have been observed in  $\text{GdCo}_9\text{Si}_4$  and  $\text{TbCo}_9\text{Si}_4$  [20, 21].

The spin-flip transition of Co and Dy magnetic moments can be observed at  $T = 20$  K as well, where the field-dependence of the sample temperature shows a weak anomaly as discussed later. For  $T > 20$  K, the transition is not clearly seen in the  $M(H)$  curve. However, in the  $dM/dH$  curve

of Fig. 6 (b), a broad anomaly around 20 T is detected even for the measurement at  $T = 40$  K. It is noted that the ferromagnetic ordering of the Co magnetic moment sets in at  $T_C = 40$  K. Thus, the weak anomaly in the  $dM/dH$  curve at  $T = 40$  K indicates that the antiparallel coupling between the Co and Dy magnetic moments is strong, persisting at high temperatures near  $T_C$ . Such a short-range antiferromagnetic coupling between Co and rare-earth magnetic moment in the paramagnetic region is reminiscent of that observed in the cubic  $\text{ErCo}_2$  and  $\text{HoCo}_2$  compounds [25, 26, 27], where the peculiar magnetic state has been referred to as ‘*Parimagnetism*’. In the case of  $\text{ErCo}_2$ , the antiparallel coupling of Er and Co magnetic moments is seen up to about  $3T_C \sim 100$  K. Above 100 K, the magnetic moments are considered to be independent [25, 26]. In addition, the existence of short-range ferromagnetic clusters was suggested for  $\text{ErCo}_2$  and  $\text{HoCo}_2$  in the ‘*Parimagnetic*’ regime by the small-angle neutron scattering [25] and  $\mu\text{SR}$  [26]. For the present case of  $\text{DyCo}_9\text{Si}_4$ , although the coupling of Dy and Co magnetic moment is seen at  $T_C = 40$  K, it is not clear if such a short-range order exists at  $T > T_C$ , since the  $dM/dH$  curves at  $T = 50$  and 60 K in Fig. 6 (b) do not show an anomaly. Therefore, the magnetism of  $\text{DyCo}_9\text{Si}_4$  at  $T > T_C$  may be understood as the conventional paramagnetic state. Even in that case, there can remain some effect of short-range correlations in the temperature range below  $3T_C = 120$  K. Thus, the Curie-Weiss fitting for the range from 150 to 300 K can be reasonable to count all the magnetic moments involved.

In Fig. 6 (c), the sample temperatures as functions of magnetic fields are shown. As described above, the magnetization measurements for  $T = 1.4$  and 4.2 K were done in a setup where the sample was placed in liquid helium. Hence, the sample temperature is almost unchanged during the magnetic field scan. On the other hand, for the measurements at  $T > 4.2$  K, the measurements were carried out in a helium gas atmosphere. In that case, the magnetization process using the pulsed field in about 36 msec can be regarded as a quasi-adiabatic magnetization process. As a result, the sample temperature increases with increasing magnetic field by the magnetocaloric effect of the sample [1]. Hence, the magnetization processes shown in Fig. 6 (a) are not isothermal magnetization precisely. This seemingly is a common event for the case of magnetization measurements in a pulsed field, and requires a careful analysis especially for materials having large magnetic degree of freedom and small heat capacity. One successful demonstration can be seen in the case of the first-order metamagnetic transition in  $\text{UTe}_2$  [19, 28]. Even for the relatively large electronic specific heat of  $\text{UTe}_2$ , the large jump in the magnetization across the metamagnetic transition causes a non-negligible magnetocaloric effect. In the present case, however, the magnetization curves above  $T = 10$  K are not sensitive to a slight difference in temperature, as one can see from Fig. 6 (a). Thus, we use the initial temperature value to label the magnetization curves.

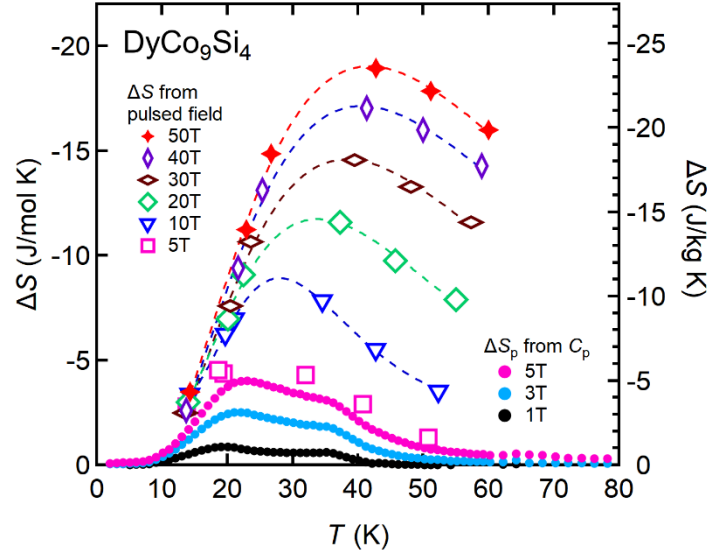


Fig. 7 Entropy change by magnetic fields  $\Delta S$  in  $\text{DyCo}_9\text{Si}_4$  as functions of temperature, obtained by the pulsed magnetic field experiments. Broken lines are guide for eye.  $\Delta S_p$  obtained from the specific heat data are also shown for comparison.

In the following, we evaluate the magnetocaloric effect in  $\text{DyCo}_9\text{Si}_4$  using the temperature change by pulsed field. If we assume the adiabatic process for the magnetization measurements above 10 K, the temperature change should be due to the iso-entropy process. This is depicted in Fig. S5 (b) in the supporting information, where the measured sample-temperature values of  $\text{DyCo}_9\text{Si}_4$  in magnetic fields are plotted at the same entropy lines. Here, the entropy values at zero magnetic field were set to those evaluated from the specific heat data. Next, the entropy changes by the pulsed magnetic fields,  $\Delta S$ , have been calculated by taking the difference and are plotted in Fig. 7 as functions of temperature. The entropy changes evaluated from the specific heat data,  $\Delta S_p$  are also plotted for comparison. The  $\Delta S$  values for the field change of 5 to 0 T obtained by temperature changes in the pulsed fields and by the specific heats are relatively in good agreement, indicating the estimation of  $\Delta S$  from the pulsed fields is accurate enough for discussion. At 5 T, the  $\Delta S$  curve has two peaks at  $T_m = 20$  K and  $T_C = 40$  K, as shown in the figure. With increasing field, the  $\Delta S$  maxima shift to higher temperatures, and the two anomalies appear to merge into single peak. This is consistent with the ferromagnetic alignment of the Co and Dy magnetic moments at high fields. The maximum value of  $\Delta S$  is seen at  $T \sim 40$  K with the magnetic field change from 50 to 0 T, where  $\Delta S = -24$  J/kg K is obtained. Here, it is notable that a similar large  $\Delta S$  value has been reported for  $\text{GdCo}_9\text{Si}_4$  as well for the field change from 5 to 0 T [14]. Although the magnetic properties of  $\text{GdCo}_9\text{Si}_4$  and  $\text{DyCo}_9\text{Si}_4$  look similar, much larger magnetic field has to be applied for the latter compound to achieve a similar  $\Delta S$  value. This may partly be due to the

existence of the orbital angular momentum in  $\text{Dy}^{3+}$ , which can cause magnetic anisotropy and the CEF splitting. Considering about these effects should be important to evaluate the magnetocaloric performances of rare-earth intermetallic compounds in general [15].

Another point to be noted in the present study is the magnetocaloric effect associated with the spin-flip transition. As shown in Fig. 6 (a), the step-like increase in the magnetization around  $H = 20$  T indicates the transition of the magnetic structure from a ferrimagnetic state with antiparallel couplings of Co and Dy magnetic moments to a ferromagnetically aligned one. For such field-induced magnetic-structure changes, a distinct magnetocaloric effect may appear like the case of Ho [29]. In the present case, however, the sample-temperature in the pulsed field (Fig. 6 (c)) shows little change around  $H = 20$  T for the  $T = 10$  K data. As a result, the calculated  $\Delta S$  (Fig. 7) almost coincides for  $H > 10$  T at  $T = 10$  and 20 K. This indicates that the spin-flip transition itself in  $\text{DyCo}_9\text{Si}_4$  does not cause a magnetocaloric effect. The difference between Ho and  $\text{DyCo}_9\text{Si}_4$  can be found in the  $M$ - $H$  process. In the former, the metamagnetic-transition field  $H_C$  depends sharply on temperature [29]. For  $\text{DyCo}_9\text{Si}_4$ , on the other hand, the  $M$ - $H$  curves almost agree below 10 K without temperature dependence, as seen in Fig. 6(a). From a macroscopic point of view, the different magnetocaloric properties of the two compounds are ascribed to these different  $M$ - $H$  behavior, since the magnetization and magnetic entropy are connected through the Maxwell's relation. Further investigation of the magnetic structure may be useful to clarify the microscopic origin of the difference and to shed light on the mechanism of the large magnetocaloric effect. Nevertheless, the large  $\Delta S$  value suggests the potential of the  $R\text{Co}_9\text{Si}_4$ -type compounds for magnetic refrigeration materials if large magnetic fields are available by using superconducting magnets, or if the molecular fields can assist the external magnetic field to induce the magnetic transition, like the case in  $R\text{Co}_2$ . Furthermore, the present results demonstrate that the pulsed-field measurement is an effective and reliable method to evaluate the magnetocaloric effect of materials.

## Conclusion

The  $R\text{Co}_9\text{Si}_4$  systems have a lot of similarities with the cubic  $R\text{Co}_2$  compounds in their magnetic properties, especially in the interplay of Co and  $R$  magnetic moments. We have for the first time synthesized a pure  $\text{DyCo}_9\text{Si}_4$  compound with the tetragonal  $\text{LaFe}_9\text{Si}_4$ -type structure by arc melting and high-temperature annealing. The magnetization measurement reveals that the Co magnetic moments participate in the Curie-Weiss paramagnetism, in addition to those of Dy ions. A ferromagnetic transition at  $T_C = 40$  K and a broad anomaly at  $T_m = 20$  K were identified by the magnetization measurements. The former is due to the itinerant electron ferromagnetism by Co ions, whereas the latter is attributed to the formation of anti-parallel coupling of Co and Dy magnetic moments. These anomalies were also confirmed by the electrical resistivity and the specific heat measurements. The magnetic entropy changes were evaluated from specific heat

data and from the magnetization data with the Maxwell relation, which showed a good agreement with each other.

The magnetization measurements up to 50 T were done with pulsed fields. The results reveal the step-like increase of the magnetization above 20 T, indicating a spin-flip transition from anti-parallel to ferromagnetic configuration of Co and Dy magnetic moments. The spin-flip behavior was observed at  $T = 40$  K. This suggests the possibility that the anti-parallel coupling of Co and Dy moments persists even around  $T_C$ , pointing to some similarity to the ‘*Parimagnetism*’ reported for  $\text{ErCo}_2$  and  $\text{HoCo}_2$ .

The magnetocaloric effect of  $\text{DyCo}_9\text{Si}_4$  was evaluated by the temperature dependent magnetization data using the Maxwell relation, by the specific heat data in magnetic fields, and also by the sample-temperature change measured with the pulsed magnetic fields. The entropy change  $\Delta S$  from 5 to 0 T evaluated by these methods almost agrees each other. The maximum value of  $\Delta S$  with the field scan from 5 to 0 T was  $-5$  J/kg K at  $T = T_m$ . The maximum  $\Delta S$  from 50 to 0 T is evaluated to be  $-24$  J/kg K. These results also suggest that the pulsed-field measurement can be a quick and reliable tool for the evaluation of the magnetocaloric effect.

### Acknowledgements

The measurements using pulsed magnetic fields were carried out at the Institute for Solid State Physics, the University of Tokyo, as a joint research with the application number 202104-HMBXX-0048. This research was supported by the Grant-in-Aid from Japan Society for the Promotion of Science (JSPS), KAKENHI, 21F21322 and 22H01761. This research was partly supported by the JST-Mirai program, JPMJMI18A3, Japan. They thank A. Kawaguchi for the help of sample preparation and characterization.

### References

- [1] K. A. Gschneidner Jr., V. K. Pecharsky, and A. O. Tsokol, *Rep. Prog. Phys.* **68**, 1479-1539 (2005).
- [2] X. Tang, H. Sepehri-Amin, N. Terada, A. Martin-Cid, I. Kurniawan, S. Kobayashi, Y. Kotani, H. Takeya, J. Lai, Y. Matsushita, T. Ohkubo, Y. Miura, T. Nakamura, and K. Hono, *Nature Commun.* **13**, 1817 (2022).  
<https://doi.org/10.1038/s41467-022-29340-2>
- [3] T. Goto, K. Fukamichi, and H. Yamada, *Physica B* **300**, 167-185 (2001).
- [4] A. Fujita, S. Fujieda, K. Fukamichi, H. Mitamura, and T. Goto, *Phys. Rev. B* **65**, 014410 (2001).  
<https://doi.org/10.1103/PhysRevB.65.014410>
- [5] S. Fujieda, A. Fujita, and K. Fukamichi, *Appl. Phys. Lett.* **81**, 1276 (2002).  
<https://doi.org/10.1063/1.1498148>

- [6] N. Tsujii, *J. Alloys Compds.* **612**, 170 (2014).  
<https://doi.org/10.1016/j.jallcom.2014.05.090>
- [7] H. Michor, M. El-Hagary, M. Della Mea, M. W. Pieper, M. Reissner, G. Hilscher, S. Khmelevskiy, P. Mohn, G. Schneider, G. Giester, and P. Rogl, *Phys. Rev. B* **69**, 081404R (2004).  
<https://doi.org/10.1103/PhysRevB.69.081404>
- [8] K. Moriyama, J. Murakawa, H. Kanagawa, C. Michioka, H. Ueda, H. Michor, and K. Yoshimura, *J. Japan Soc. Powder Powder Metallurgy* **69**, 467-474 (2022).  
<https://doi.org/10.2497/jjspm.69.467>
- [9] H. Michor, M. El-Hagary, S. Özcan, A. Horyn, E. Bauer, M. Reissner, G. Hilscher, S. Khmelevskiy, P. Mohn, and P. Rogl, *Physica B* **359-361**, 1177-1179 (2005).
- [10] M. El-Hagary, H. Michor, E. Bauer, R. Grössinger, P. Kersch, D. Eckert, K. -H. Müller, P. Rogl, G. Giester, and G. Hilscher, *Physica B* **359-361** (2005) 311-313.
- [11] M. El-Hagary, *Eur. Phys. J. Appl. Phys.* **42**, 287-291 (2008).  
<https://doi.org/10.1051/epjap:2008088>
- [12] M. El-Hagary, H. Michor, E. Bauer, M. Della Mea, K. Hense, and G. Hilscher, *J. Mag. Mag. Mater.* **272-276**, e445 (2004).  
<https://doi.org/10.1016/j.jmmm.2003.12.1164>
- [13] N. Mohapatra and E. V. Sampathkumaran, *Solid State Commun.* **145**, 507-511 (2008).  
<https://doi.org/10.1016/j.ssc.2007.12.008>
- [14] M. El-Hagary, H. Micho, and G. Hilscher, *J. Mag. Mag. Mater.* **322**, 2840-2844 (2010).  
<https://doi.org/10.1016/j.jmmm.2010.04.039>
- [15] N. Terada, H. Mamiya, H. Saito, T. Nakajima, T. D. Yamamoto, K. Terashima, H. Takeya, O. Sakai, S. Itoh, Y. Takano, M. Hase, and H. Kitazawa, *Commun. Mater.* **4**, 13 (2023).  
<https://doi.org/10.1038/s43246-023-00340-z>
- [16] M. Q. Huang, W. E. Wallace, R. T. Obermyer, S. Simizu, M. McHenry, and S. G. Sankar, *J. Appl. Phys.* **79**, 5949-5951 (1996).
- [17] Y. Gorelenko, R. Matviishyn, I. Shcherba, V. Pavlyuk, and R. Serkiz, *Chem. Met. and Alloys* **2**, 18-24 (2009).
- [18] A. Miyake, H. Mitamura, S. Kawachi, M. Tokunaga, K. Kimura, T. Kimura, T. Kihara, and M. Tachibana, *Rev. Sci. Instrum.* **91**, 105103 (2020).  
<https://doi.org/10.1063/5.0010753>
- [19] A. Miyake, Y. Shimizu, Y. J. Sato, D. Li, A. Nakamura, Y. Homma, F. Honda, J. Flouquet, M. Tokunaga, and D. Aoki, *J. Phys. Soc. Japan* **90**, 103702 (2021).  
<https://doi.org/10.7566/JPSJ.90.103702>
- [20] M. E. Hagary, H. Michor, S. Özcan, M. Giovannini, A. Matar, Z. Heiba, P. Kersch, M. Schönhart, E. Bauer, R. Grössinger, G. Hilscher, J. Freudenberger, and H. Rosner, *J. Phys.:*

*Condens. Matter* **18**, 4567 (2006).

<http://dx.doi.org/10.1088/0953-8984/18/19/011>

[21] R. Grössinger, M. Schönhart, P. Kersch, S. Özcan, M. E. Hagary, J. Freudenberger, and H. Micho, *J. Phys.: Conf. Ser.* **51**, 139 (2006).

doi:10.1088/1742-6596/51/1/031

[22] D. Lamago, R. Georgii, and P. Böni, *Physica B* **359-361**, 1171-1173 (2005).

<https://doi.org/10.1016/j.physb.2005.01.317>

[23] T. Kiyama, K. Yoshimura, K. Kosuge, H. Michor, and G. Hilscher, *J. Phys. Soc. Japan* **67**, 307-311 (1998).

<https://doi.org/10.1143/JPSJ.67.307>

[24] K. Sato, T. Naka, M. Taguchi, T. Nakane, F. Ishikawa, Y. Yamada, Y. Takaesu, T. Nakama, A. de Visser, and A. Matsushita, *Phys. Rev. B* **82**, 104408 (2010).

<http://dx.doi.org/10.1103/PhysRevB.82.104408>

[25] J. H-Albillos, F. Bartolomé, L. M. García, J. Campo, and G. J. Cuello, *Phys. Rev. B* **76**, 094409 (2007).

<http://dx.doi.org/10.1103/PhysRevB.76.094409>

[26] C. M. Bonilla, N. Marcano, J. H-Albillos, A. Maisuradze, L. M. García, and F. Bartolomé, *Phys. Rev. B* **84**, 184425 (2011).

<https://doi.org/10.1103/PhysRevB.84.184425>

[27] J. Valenta, J. Prchal, R. Khasanov, M. Kratochvílová, M. Míšek, M. Vališka, and V. Sechovsky, *J. Phys.: Conf. Ser.* **500**, 182041 (2014).

<https://iopscience.iop.org/article/10.1088/1742-6596/500/18/182041>

[28] A. Miyake, M. Gen, A. Ikeda, K. Miyake, Y. Shimizu, Y. J. Sato, D. Li, A. Nakamura, Y. Homma, F. Honda, J. Flouquet, M. Tokunaga, and D. Aoki, *J. Phys. Soc. Japan* **91**, 063703 (2022).

<https://doi.org/10.7566/JPSJ.91.063703>

[29] N. Terada and H. Mamiya, *Nature Commun.* **12**, 1212 (2021).

<https://doi.org/10.1038/s41467-021-21234-z>